



Dry citrate-precursor synthesized nanocrystalline cobalt oxide as highly active catalyst for total oxidation of propane

Qian Liu, Lu-Cun Wang, Miao Chen, Yong Cao*, He-Yong He, Kang-Nian Fan

Department of Chemistry and Shanghai Key Laboratory of Molecular Catalysis and Innovative Materials, Fudan University, Shanghai 200433, PR China

ARTICLE INFO

Article history:

Received 12 November 2008
Revised 27 January 2009
Accepted 27 January 2009
Available online 12 February 2009

Keywords:

Propane
Total oxidation
Nanocrystalline Co_3O_4
Electrophilic oxygen
Lattice distortion

ABSTRACT

A set of nanocrystalline cobalt oxide (Co_3O_4)-based catalysts have been prepared by means of an innovative soft reactive grinding (SRG) procedure. The catalysts exhibited excellent activities and high stabilities for propane catalytic combustion. Complete conversion has been achieved at reaction temperatures as low as 240 °C. Comparing with the highly active Co_3O_4 catalysts in the current literature, the catalysts in this work show exceptionally high specific rate for propane total oxidation (ca. 91.3 $\text{mmol}_{\text{C}_3}\text{m}^{-2}\text{h}^{-1}$ at 200 °C). A correlation between the O_2 -TPD results and the activity for Co_3O_4 reveals that a high concentration of superficial electrophilic oxygen (O^-) species is important for achieving a high activity. The prominent lattice distortion induced by prolonged citrate-precursor grinding is suggested to play a key role in creating and maintaining a high density of surface defects, which leads to highly activity and stability of the cobalt spinel catalyst.

© 2009 Elsevier Inc. All rights reserved.

1. Introduction

Catalysts based on cobalt oxides are of great importance for catalytic processes like Fischer–Tropsch synthesis [1,2], low-temperature CO oxidation [3,4], N_2O decomposition [5], steam reforming of ethanol [6] and other industrially important hydrogenation and oxidation reactions [7,8]. It is also established that such materials are effective combustion catalysts for VOC removal [9], diesel soot oxidation [10], and particularly total oxidation of light hydrocarbons [11,12], which has recently emerged as promising process for environmentally benign energy generation and emissions control. As a result, cobalt oxides and their preparation have been extensively studied [13,14]. The high catalytic activity in reactions oxygen involving of the Co_3O_4 -based catalysts is most likely related to the high bulk oxygen mobility [15] and facile formation of highly active electrophilic oxygen (O^- or O_2^-) species for hydrocarbon oxidation [16].

Currently, several methods are used for the synthesis of cobalt oxide catalysts [13–18]. Among them, coprecipitation routes via the hydroxycarbonate precursors are popular [17]. However, the shortcoming of the coprecipitation routes is the need of subsequent calcination at temperatures higher than 350 °C to induce the full decomposition of the basic cobalt(II) carbonate precursor, which however leads to undesirable sintering, grain growth, and dramatic loss of specific surface area in many cases [17]. Another limitation

of this wet chemical method is the use of vast amounts of water as well as formation of large amounts of gaseous or liquid wastes, which presents additional environmental problems [18]. In view of these circumstances, the development of new practical and environmental friendly synthetic methods for preparation of a high surface area cobalt oxide catalyst system is highly desirable.

Over the last decade, increasing attention has been paid to the catalytic combustion of light alkanes, especially of propane, with the aim of providing new technological solutions towards more efficient energy production while simultaneously reducing emissions from liquid petroleum gas powered vehicles [19,20]. In view of its application, catalysts with high activity and stability are needed [19,21]. A great number of platinum group metal (PGM)-based catalysts with various modifications have been tested [22,23]. However, the development of a versatile material that can allow efficient oxidation of propane at lower temperatures still remains a major challenge. Recently, Solsona et al. focused on the design and evolution of base-metal oxides which exhibits enhanced low temperature activities [19,24], and found that nanocrystalline Co_3O_4 with high surface area (ca. 99 m^2g^{-1}) are highly active for total oxidation of propane [24]. The excellent combustion activity has been attributed to the enhanced reducibility of the nanocrystalline Co_3O_4 catalyst, which was found to be critically dependent on the crystallite size of the cobalt oxides.

In continued search for more effective technologies for propane combustion, there is a definite need for new improved cobalt oxide-based catalysts that can allow more efficient total oxidation of propane. In the present work, we report the development of new efficient high surface area nanocrystalline Co_3O_4 system

* Corresponding author. Fax: +86 21 65642978.

E-mail address: yongcao@fudan.edu.cn (Y. Cao).

Table 1
Physicochemical properties of various Co₃O₄ catalysts.

Catalysts	S_{BET} (m ² g ⁻¹)		d_{XRD} (nm)	Lattice parameter (Å)	Microstrain ^b (%)	Temperature of α_2 position (°C)	$A\alpha_1/A\alpha_2^c$	B.E. ^d (eV)
	Fresh	After reaction ^a						
Co ₃ O ₄ -SG	55	51	23	8.0769	0.101	390	–	529.4/531.4 (16%)
Co ₃ O ₄ -CC	53	50	21	8.0752	0.104	340	–	529.3/531.4 (12%)
Co ₃ O ₄ -GC-0.5	112	110	13	8.0690	0.203	265	1.784/1.017	529.5/531.2 (54%)
Co ₃ O ₄ -GC-1	115	113	14	8.0661	0.236	265	2.127/2.144	529.5/531.2 (60%)
Co ₃ O ₄ -GC-3	119	117	13	8.0645	0.276	265	1.907/3.154	529.5/531.2 (68%)
Co ₃ O ₄ -GC-6	120	118	12	8.0631	0.303	265	1.349/3.672	529.4/531.1 (78%)

^a S_{BET} data measured after the light-off test as a function of temperature for propane combustion over Co₃O₄ samples (200 mg catalyst, space velocity of 0.12 g s mL⁻¹).

^b The microstrain of the Co₃O₄ crystals estimated from the X-ray diffraction lines.

^c The fitted area from O₂-TPD of peak α_2 ($A\alpha_2$) or α_1 ($A\alpha_1$).

^d Binding energy of surface lattice oxygen and O⁻ species. Data in parenthesis is the relative amount of surface O⁻ (%) extracted from XPS data.

exhibiting enhanced activity and stability for total oxidation of propane. Soft reactive grinding (SRG) based on mechanochemical activation [25,26], previously established to be an effective and easily-scalable technique for a nitrate-free preparation of nanostructured Cu/ZnO catalysts highly efficient for methanol steam reforming (MSR) by our group [27], has shown to be particularly useful in preparing a highly active Co₃O₄ for propane combustion. Our results have shown that the SRG technique based on dry citrate-precursor synthesis can allow the favorable creation of highly strained Co₃O₄ nanocrystals, which makes the cobalt spinel catalysts highly active and stable for the reaction.

2. Experimental

2.1. Catalyst preparation

Three types of Co₃O₄ samples were prepared by different dry and wet-chemical synthesis methods, i.e. soft reactive grinding of citric acid with the Co(II) basic carbonate precursors (Co₃O₄-GC); aqueous coprecipitation via the hydroxycarbonate precursors (Co₃O₄-CC); aqueous sol-gel citrate procedure based on citric acid-complexation (Co₃O₄-SG). The detailed synthesis procedures are described below.

A typical procedure to prepare the Co₃O₄-GC catalysts is as follows: 1.33 g 2CoCO₃·3Co(OH)₂·H₂O (purchased from Aldrich) and 2.17 g C₆H₈O₇ (citric acid; from Aldrich) were premixed by hand grinding for ca. 5 min. The mixed powder was then loaded into a plastic vial (50 mL) with agate milling balls (3–5 mm) under air atmosphere. The weight ratio of the balls to powders was 10:1. The grinding was carried out in a planetary mill (QM-1SP04) at a speed of 600 rpm for 0.5, 1, 3, and 6 h. After the completion of grinding, the as-ground citrate precursor (produced via the solid-state displacement reaction of citric acid with cobalt salts) was separated from the balls followed by calcination at 300 °C in air for 4 h. The final calcined samples were designated as Co₃O₄-GC-*t*, where *t* stands for the grinding time (see Table 1).

For comparison, two reference Co₃O₄ catalysts obtained by the wet-chemical methods were prepared. Briefly, the Co₃O₄-CC catalyst was prepared by aqueous hydroxycarbonate coprecipitation according to a method described elsewhere [17]. A 1.2 M aqueous solution of NaCO₃ was added into an aqueous solution of cobalt nitrates (each 0.5 M) under vigorous stirring. The temperature was kept at 80 °C during precipitation and maintaining the pH at 8.5. The precipitates were washed thoroughly and dried in air at 110 °C for 12 h, followed by calcination at 350 °C in air for 4 h. The Co₃O₄-SG catalyst was prepared by a well-established aqueous sol-gel citrate procedure involving complexation of cobalt nitrate and citric acid according to a method described in Ref. [6]. An excess citric acid was used to ensure complete complexation. The mixture was dried at 110 °C and the resulting citrate was calcined at 300 °C in air for 4 h.

2.2. Characterization of catalysts

The BET specific surface areas of the calcined catalysts were determined by adsorption-desorption of nitrogen at liquid nitrogen temperature, using a Micromeritics TriStar 3000 equipment. The images of scanning electron microscope (SEM) were obtained using a Philips XL 30 microscope operating at 30 kV. Images of transmission electron microscopy (TEM) were recorded on a JEOL 2011 electron microscope operating at 200 kV. X-ray photoelectron spectroscopic (XPS) data were obtained with a Perkin-Elmer PHI 5000C system equipped with a hemispherical electron energy analyzer. The carbonaceous C1s line (284.6 eV) was used as the reference to calibrate the binding energies (BE).

The X-ray powder diffraction (XRD) was carried out on a Bruker AXS D8 Avance X-ray diffractometer with nickel filtered CuK α radiation, with a step width of 0.02° and 5 s per step. The lattice parameters calculated by the square method according to the Cohen procedure [28]. The crystallite size corresponding to the broadening of each *hkl* line was determined from the Lorentzian part of the individual profile functions, while the microstrain was determined from the Gaussian part [29]. The laser Raman spectra were obtained at room temperature using a confocal microprobe Jobin Yvon Lab Ram Infinity Raman system with a spectral resolution of 2 cm⁻¹. The internal 514.5 nm line from Ar⁺ excitation with a power of 10 mW was used as the source.

Temperature-programmed reduction (TPR) profiles were obtained on a homemade apparatus as described elsewhere [30]. The total flow rate of the feed (5 vol% H₂/Ar) was 40 mL min⁻¹. Before experiment the sample (20 mg) was preheated in a stream of air at 200 °C for 30 min, and then cooled to room temperature. The sample was heated at a ramping rate of 5 °C min⁻¹ to a final temperature of 600 °C. The H₂ consumption was monitored using a TCD detector. Temperature-programmed desorption (TPD) of O₂ was also carried out in the fixed-bed flow reactor. The catalyst (200 mg) was pretreated in helium at 300 °C for 1 h, then the oxygen adsorption was proceeded with 20 vol% O₂/He at 200 °C for 0.5 h. After cooling to room temperature, the system was purged in He (60 mL min⁻¹) for 1 h. After the treatment, the temperature was raised to 800 °C at a rate of 10 °C min⁻¹ in the helium flow (60 mL min⁻¹), and the effluent gases from the reactor were analyzed with a Balzers Omnistar benchtop mass spectrometer.

2.3. Catalyst activity tests and kinetic measurements

The catalysts were evaluated at atmospheric pressure using a fixed bed quartz reactor. The sample (200 mg) was diluted with 1.0 g of SiC (60–80 mesh). Before reaction, the catalysts were pretreated with air (30 mL min⁻¹) at 200 °C for 0.5 h. The feed was a mixture of 1 vol% propane, 10 vol% O₂, and 89 vol% N₂ with a total flow rate of 100 mL min⁻¹, corresponding to a W/F of 0.12 g s mL⁻¹. The temperature of reaction, coaxially measured

with a thermocouple, was increased from 180 °C to total conversion of propane, at intervals of 10 °C. The data obtained at each temperature were the average of three steady-state measurements. Kinetic measurements were performed under differential reaction conditions, with typically 20 mg catalyst powder. In order to limit the conversion to values typically between 5 and 20%, the catalyst samples were diluted with chemically inert SiC. Kinetic data were also acquired after 60 min reaction time. The hydrocarbon reaction products were analyzed by gas chromatography (Type GC-122, Shanghai) on line equipped with a 6-m packed column of Porapak Q and a flame ionization detector. The permanent gas products were analyzed online by another gas chromatograph equipped with a TDX-01 column and a TCD. The differences between the inlet and outlet concentrations were used to calculate conversion data. No carbon containing product of oxidation other than CO₂ has been detected, which was further confirmed by carbon balance on propane and CO₂ with an accuracy of ±2%. Blank experiments were conducted in an empty reactor which showed negligible activity over the temperature range used in this work.

3. Results and discussion

3.1. Structural and textural characterization

The BET specific surface areas (S_{BET}) of all of the grinding-derived catalyst series, measured before and after catalytic testing, are given in Table 1. The S_{BET} of wet-chemically derived Co₃O₄-CC and Co₃O₄-SG are also shown as references. It is shown that all the four Co₃O₄-GC samples show large specific surface areas exceeding 110 m² g⁻¹, suggesting the effectiveness of this method for the synthesis of metal oxides possessing high specific surface area. In contrast, the surface areas measured for the wet-chemically derived reference samples are significantly lower than the Co₃O₄-GC samples. Moreover, the grinding-derived samples reveal a quite similar surface area of these materials, pointing to a weak relationship between the grinding time and the textural properties of the Co₃O₄-GC materials. It is interesting to note that a significantly different variation behavior of the surface area as a function of the grinding time has been observed in the grinding-assisted preparation of Cu/Zn mixed oxides [27]. Although there is a trend of decreasing surface area after reaction, the small change is in the range of experimental error. Therefore, the surface area may be considered remaining the same.

Fig. 1 shows the XRD patterns of the cobalt oxide catalysts obtained with various methods. The only pure cobalt phase identified was the spinel structured Co₃O₄. No diffraction peaks related to a CoO phase were detected. The Co₃O₄ diffraction lines shows that all Co₃O₄-GC samples give a much broader profile with respect to the reference samples, in line with the much higher specific surface area as observed for the formers. The average crystallite sizes of Co₃O₄ as shown in Table 1 reveal a much smaller particle size for Co₃O₄-GC (ca. 13 nm) as compared to Co₃O₄-CC (21 nm) and Co₃O₄-SG (23 nm). Note that no obvious influence of the grinding activation on the particle size was identified for the Co₃O₄-GC sample series. This contrasts with the continuous decrease of CuO and ZnO particle sizes due to prolonged oxalate-precursor activation as observed in the case for preparing Cu/Zn mixed oxides [27]. The results suggest a quite different behavior of the citrate-precursor-based SRG technique in the synthesis of cobalt oxide.

On the other hand, a close comparison of the profile for Co₃O₄-GC samples with those for Co₃O₄-CC and Co₃O₄-SG catalysts in the inset to Fig. 1 reveals that the reference catalysts presents the diffraction peaks at lower angles, hence greater d-spacing, than the grinding-derived catalysts (especially Co₃O₄-GC-6). A pronounced modification of the unit-cell parameter a , within the range 8.0690–8.0631 Å, may be observed for the grinding-derived

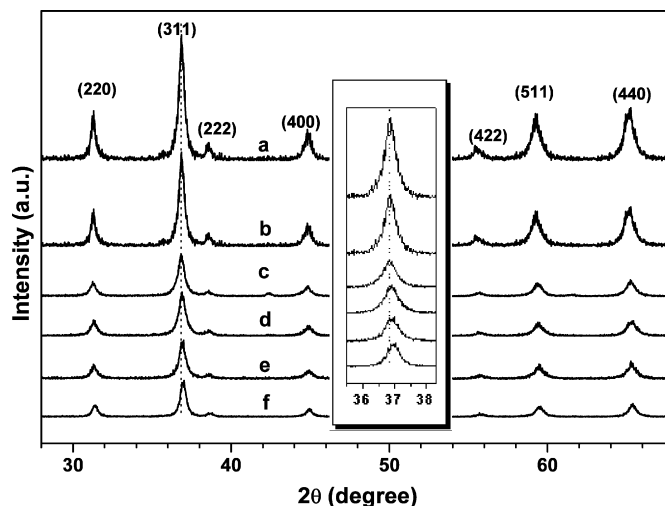


Fig. 1. XRD patterns of various Co₃O₄ catalysts. (a) Co₃O₄-SG, (b) Co₃O₄-CC, (c) Co₃O₄-GC-0.5, (d) Co₃O₄-GC-1, (e) Co₃O₄-GC-3, (f) Co₃O₄-GC-6.

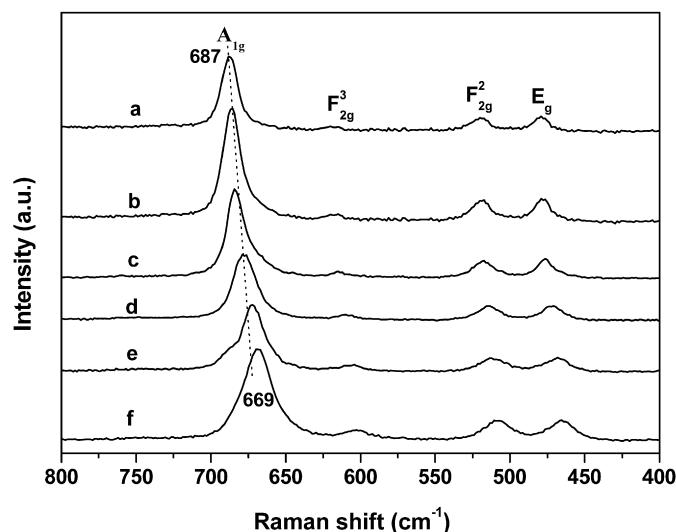


Fig. 2. Raman spectra of various Co₃O₄ catalysts. (a) Co₃O₄-SG, (b) Co₃O₄-CC, (c) Co₃O₄-GC-0.5, (d) Co₃O₄-GC-1, (e) Co₃O₄-GC-3, (f) Co₃O₄-GC-6.

samples (Table 1). It is interesting that the longer the grinding times the higher contraction of the lattice parameters. Conversely, a monotonous increase of the microstrain values is observed for the Co₃O₄-GC samples. This indicates the presence of a high degree of lattice distortion in the grinding-derived cobalt spinels. A similar microstructural modification due to an increased portion of point defects has already been reported by Lopes et al. for Co₃O₄ nanoparticles of different sizes confined in mesoporous SBA-15 materials [31]. Thus, it can be concluded that highly strained Co₃O₄ nanocrystals with enhanced structural disorder could be readily obtained in this study.

The existence of a grinding-induced lattice distortion is further confirmed by the Raman measurements. This technique has been extensively used to gain information on the structural nature of spinel crystals [32]. As shown in Fig. 2, four Raman bands at ca. 480, 520, 619 and 687 cm⁻¹, corresponding respectively to the E_g, F_{2g}¹, F_{2g}² and A_{1g} modes of the Co₃O₄ spinel structure [33], are observed for all samples. Systematic investigations of the effect of cations and isomorphous isotopic substitutions in spinels have shown that vibration with the 687 cm⁻¹ is characteristic of the sublattice (octahedral/tetrahedral) in which the highest valency cations are mainly located [33]. Any slight differences of

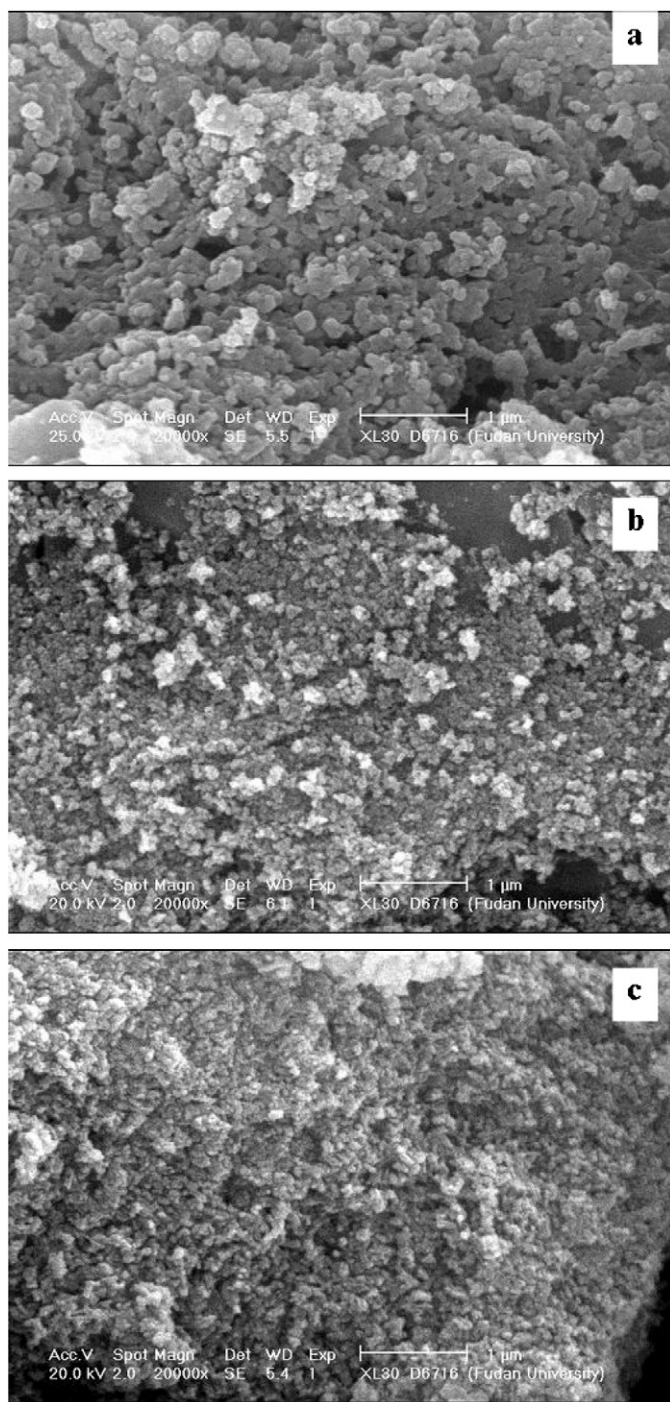


Fig. 3. SEM images of the catalysts: (a) Co_3O_4 -SG, (b) Co_3O_4 -CC, (c) Co_3O_4 -GC-6.

this vibration can be associated with lattice distortion or residual stress of the spinel structure [31]. From Fig. 2, one can see that the A_{1g} vibration shifts toward lower frequencies when the grinding time is prolonged. In addition, a significant increase in the full width at half-maximum of this band is also identified. All these facts, together with the XRD data, strongly indicate that the dry citrate-precursor synthesis procedure may be used to prepare cobalt spinel catalysts with a highly defective structure.

The morphological properties of the catalysts are investigated by SEM and TEM as shown in Figs. 3 and 4, respectively. From the SEM images in Fig. 3, the grinding-derived catalyst particles seem to be practically uniform with average size less than 100 nm. In contrast, the samples obtained by conventional wet-chemical

methods, Co_3O_4 -CC and Co_3O_4 -SG, have much larger particle size of about 300 and 400 nm. The low-magnification TEM analysis as shown in Fig. 4 further clarifies that the samples prepared with SRG approach has much smaller Co_3O_4 particles with uniform size distribution. In addition, high-resolution TEM revealed the presence of a large number of point defects on the surface of Co_3O_4 -GC-6. Therefore, both SEM and TEM results suggest that the SRG technique could be more effective than the conventional wet chemical methods in terms of the preparation of nanocrystalline cobalt oxide with improved structural properties.

3.2. Redox behaviors, O_2 -TPD and XPS studies

Fig. 5 compares the reduction behavior of all the catalysts. With respect to the reduction steps of Co_3O_4 , it is generally rather controversial in literature. Arnoldy and Moulijn [34] observed a single step for the reduction of Co_3O_4 , while many others [35–37] reported that the reduction of Co_3O_4 is a two-step process, involving the intermediate reduction to CoO. The results here clearly show two distinct reduction features at temperatures lower than 450 °C, irrespective of the preparation method, with the intensity of the first signal being significantly lower than the second one, which is consistent with the reduction behavior of fine particles of Co_3O_4 [38]. According to the literature [39], the first step is associated with the reduction of Co^{3+} ions to Co^{2+} with the concomitantly structural change to CoO, while the second step is due to the subsequent reduction of CoO to metallic cobalt. Of all the catalysts investigated, the sol-gel-derived Co_3O_4 -SG catalyst shows the highest main reduction peak. A close comparison of the various Co_3O_4 -GC samples revealed that the reductive behavior is essentially the same for all grinding-derived samples, in particular the low temperature reduction feature of these materials.

O_2 -TPD experiments have been carried out to gain an insight into the nature of the surface oxygen species that may be involved in propane combustion. According to the literature [40], the desorption peaks at temperature lower than 400 °C are generally ascribed to superficial oxygen species weakly bound to the surface. Such species are known to participate in oxidation reactions by means of a suprafacial mechanism [41]. As shown in Fig. 6, besides the reference samples, all grinding-derived samples display two prominent characteristic peaks centered around 200 and 270 °C. The first peak, often referred to α_1 -oxygen, is ascribed to physically adsorbed oxygen or $\text{O}_2^-(\text{ad})$ species [37]. The second peak, α_2 -oxygen, is associated with the desorption of O^- species [41]. It is revealed that the amount of oxygen released from Co_3O_4 -GC catalysts is much higher than that of conventional coprecipitation-derived Co_3O_4 -CC and so-gel prepared Co_3O_4 -SG samples. This is in accordance with the XRD and Raman results discussed above, most likely due to the presence of a higher density of lattice defects and a higher surface area of Co_3O_4 -GC than of reference samples.

A phenomenon worthy of note in O_2 -TPD is that for Co_3O_4 -GC catalysts prepared by SRG method, with increasing time of precursor grinding, not only the total amount of released oxygen is increased, but a significant evolution of the α_2 -peak is identified, as shown in Fig. 6(c–f). The integrated area of oxygen desorbed, calculated from deconvoluted oxygen peaks, is given in Table 1. While a less straightforward relationship was observed between grinding time and the overall superficial oxygen amount among the Co_3O_4 -GC oxides, there is a correlation between the peak area of α_2 signals and the lattice distortion based on the XRD data. The results given in Fig. 7 show that the amount of the O^- is an approximately linear function of the lattice microstrain. This result, in conjunction with much higher population of α_2 species, suggests the essential role of lattice distortion in creating a high abundance of O^- species. This type of oxygen is likely the key species to be

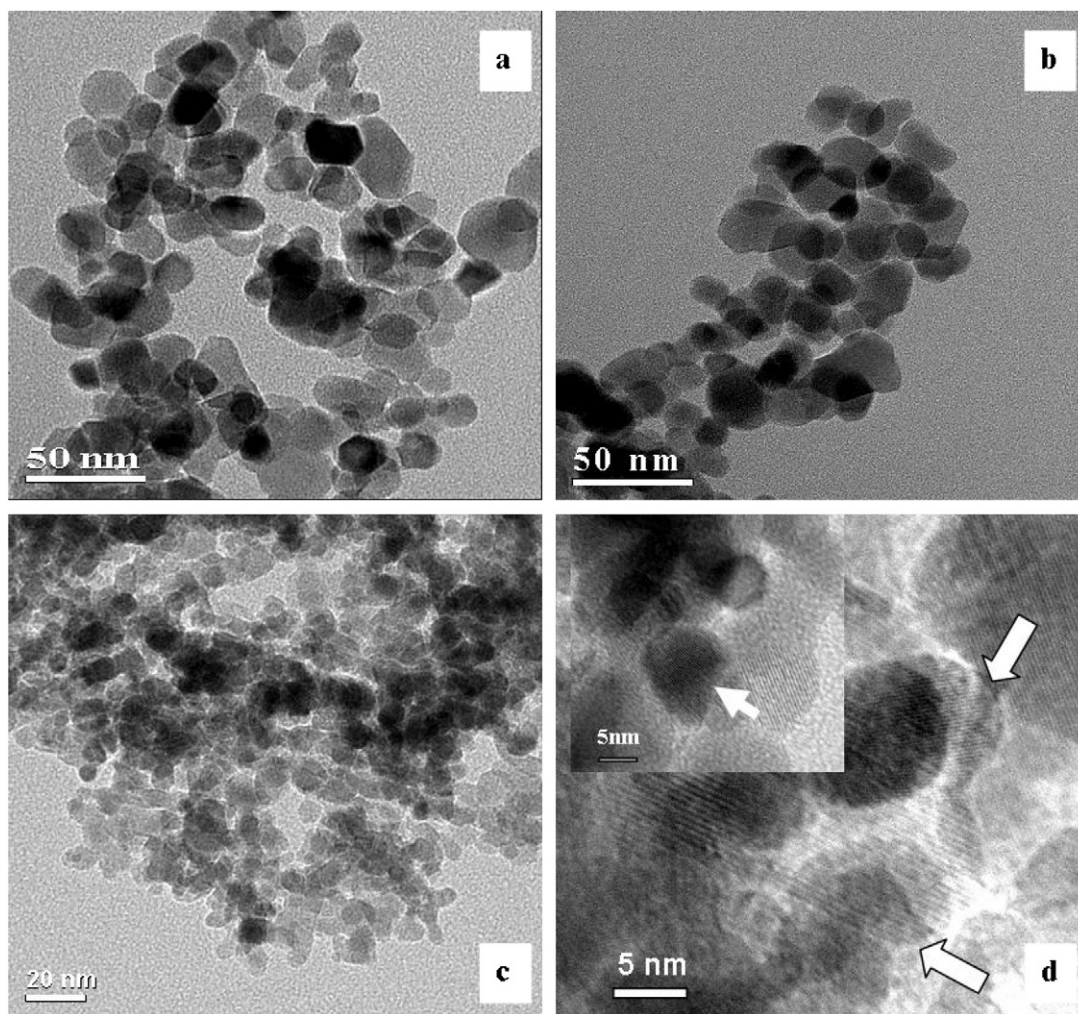


Fig. 4. TEM micrographs of (a) $\text{Co}_3\text{O}_4\text{-SG}$, (b) $\text{Co}_3\text{O}_4\text{-CC}$, (c) $\text{Co}_3\text{O}_4\text{-GC-6}$ and HR-TEM of (d) $\text{Co}_3\text{O}_4\text{-GC-6}$.

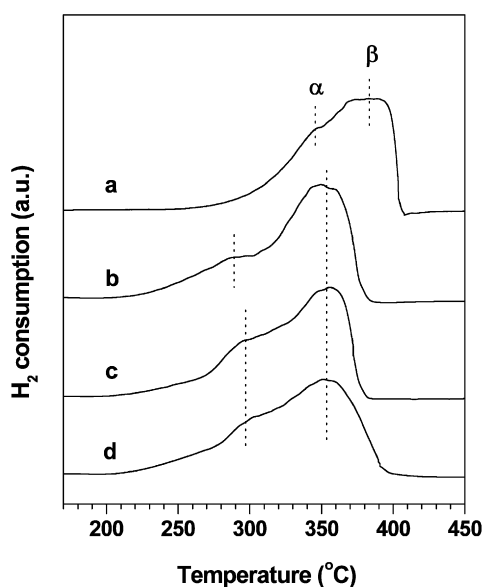


Fig. 5. TPR profiles of various Co_3O_4 catalysts. (a) $\text{Co}_3\text{O}_4\text{-SG}$, (b) $\text{Co}_3\text{O}_4\text{-CC}$, (c) $\text{Co}_3\text{O}_4\text{-GC-1}$, (d) $\text{Co}_3\text{O}_4\text{-GC-6}$.

involved in the propane oxidation, through a suprafacial mechanism.

XP spectroscopy has been employed to gain further insight into the population of the oxygen species present on the surface of the $\text{Co}_3\text{O}_4\text{-GC}$ samples. As shown in Fig. 8, a broad peak is identified for the O1s spectra of all samples, indicating the existence of several kinds of surface oxygen species which differ in their chemical states [42]. The deconvolution results are listed in Table 1. The species at binding energies of ca. 529.4 and 531.2 eV as measured for all samples are attributable to lattice O^{2-} and surface O^- species, respectively [43–45]. It is important to remark that in contrast to the reference catalysts on which surface lattice oxygen identified as the main surface oxygen species, surface O^- is clarified as the predominant surface species over all grinding-derived materials. There is an immediate correlation between the observed surface concentrations of the electrophilic oxygen species and the relative amount of O^- species measured from $\text{O}_2\text{-TPD}$. One may recall that XPS is sensitive to only the outermost ca. 20 Å of the solid, i.e. the spectra describe only the surface properties of the systems. Therefore, in combination of the $\text{O}_2\text{-TPD}$ data, the XPS results strongly suggest that the superficial oxygen species exists mainly as electrophilic O^- on the surface of the $\text{Co}_3\text{O}_4\text{-GC}$ catalysts.

3.3. Propane oxidation activity and reaction kinetics

Fig. 9 shows the catalytic performance for propane oxidation of the $\text{Co}_3\text{O}_4\text{-GC}$ catalysts, as well as the cobalt oxide catalysts

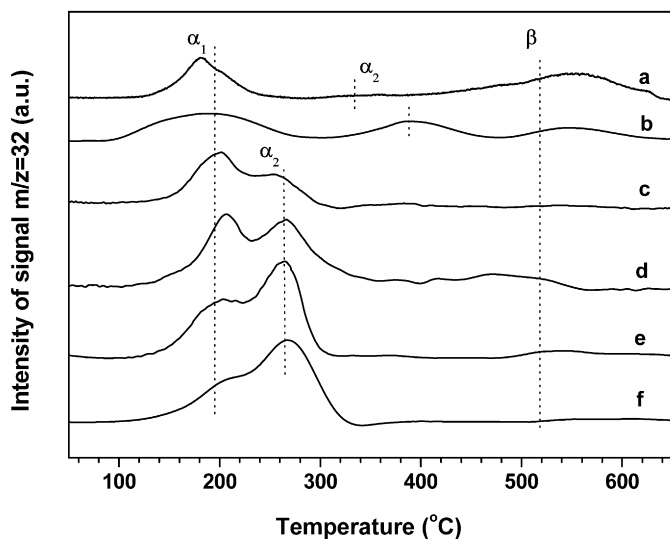


Fig. 6. Temperature-programmed desorption spectra of oxygen ($m/e = 32$) from a series of catalysts. (a) Co_3O_4 -SG, (b) Co_3O_4 -CC, (c) Co_3O_4 -GC-0.5, (d) Co_3O_4 -GC-1, (e) Co_3O_4 -GC-3, (f) Co_3O_4 -GC-6.

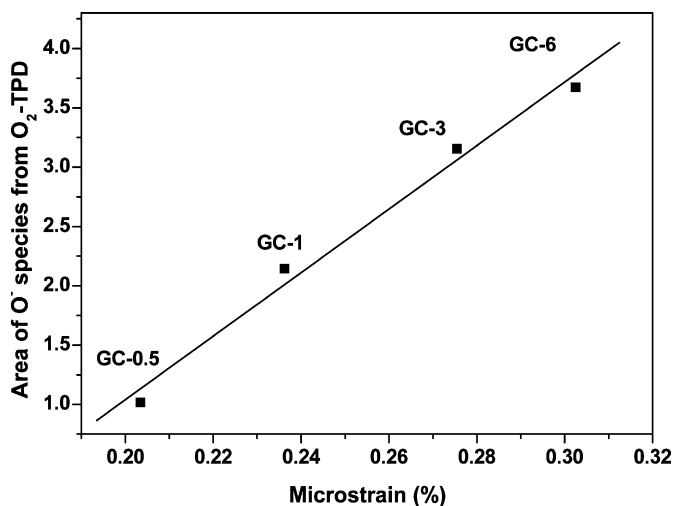


Fig. 7. Microstructural parameters and the integrated area of peak α_2 fitted from O_2 -TPD results.

derived from a conventional wet-chemical method for comparison. In Table 2, the temperatures at 10% and 100% conversion (T_{10} and T_{100}) over different catalysts are listed. For all the catalysts, no carbon containing product of oxidation other than carbon dioxide has been detected. The presence of only carbon dioxide was further confirmed by carbon balance with an accuracy better than $100 \pm 2\%$ in all cases. This very important characteristic has practical implications for potential use of nanocrystalline Co_3O_4 contrasts with NiO or Fe_2O_3 , over which significant quantities of partial propane oxidation by-products such as propylene and traces of propanol were reported [46]. The temperatures corresponding to 10 and 100% conversion (T_{10} and T_{100}) of all Co_3O_4 -GC samples are observed to be much lower than those of the reference samples. Particularly, it is seen that Co_3O_4 -GC-6 exhibited the highest performance in terms of propane combustion as compared to other samples, i.e., a half conversion temperature (T_{50}) as low as 200°C and a total conversion temperature below 240°C can be achieved over the Co_3O_4 -GC-6 catalyst.

The excellent activity of the Co_3O_4 -GC-6 material can be further seen from Table 3, where a comparison of the reaction rate per cobalt oxide mass unit as well as the areal specific activity based

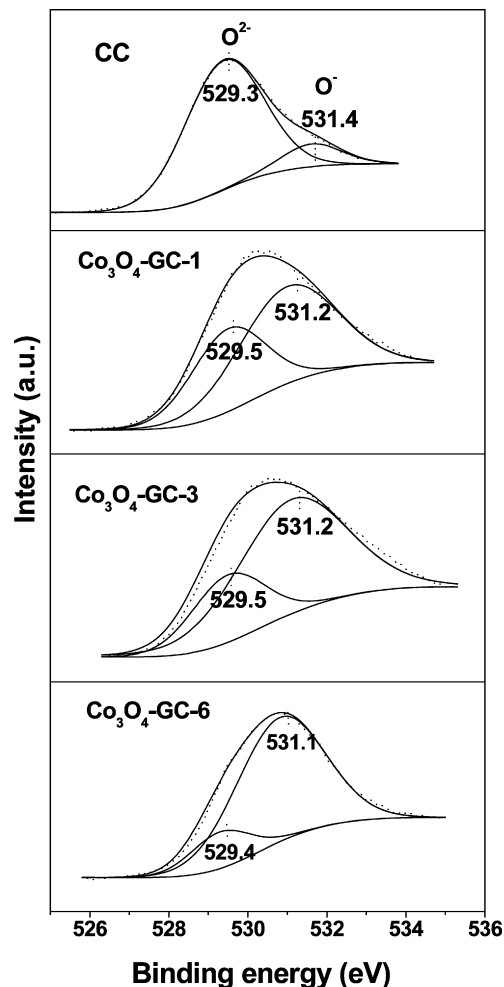


Fig. 8. O1s XPS spectra of various Co_3O_4 samples. The dotted lines describe the measured spectra, the dashed lines show the Shirley background, and the solid lines represent the individual peaks fitted to the spectra.

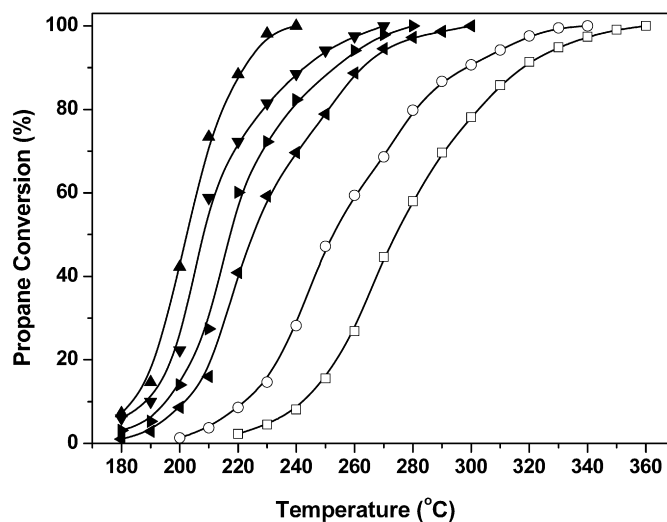


Fig. 9. Catalytic activity in total oxidation of propane as a function of the reaction temperature. (\square) Co_3O_4 -SG, (\circ) Co_3O_4 -CC, (\blacktriangleleft) Co_3O_4 -GC-0.5, (\blacktriangleright) Co_3O_4 -GC-1, (\blacktriangledown) Co_3O_4 -GC-3, (\blacktriangle) Co_3O_4 -GC-6.

on the specific surface area of the grinding-derived nanocrystalline Co_3O_4 for propane combustion with a range of cobalt oxide catalysts (including both bulk and supported cobalt oxides) has been made. It may be noted that the experimental conditions in the

literatures concerning the total oxidation of propane may deviate from each other. Nevertheless, a rough comparison is still feasible. One can see that the $\text{Co}_3\text{O}_4\text{-GC-6}$ catalyst was highly active below 240°C with an areal specific activity of $91.3 \text{ mmol}_{\text{C}_3} \text{ m}^{-2} \text{ h}^{-1}$ at 200°C . This value is significantly higher than the best cobalt-based combustion catalysts reported to date [24], demonstrating that the $\text{Co}_3\text{O}_4\text{-GC}$ in this study is very promising in hydrocarbon combustion. It is also interesting to make a further comparison of the activity of $\text{Co}_3\text{O}_4\text{-GC-6}$ with other superior materials reported to be highly active for propane combustion. For example, in a mixture of 1% propane and 16% oxygen in helium passing at 30 mL min^{-1} over 0.2 g $4.8 \text{ wt\% Pt/Al}_2\text{O}_3$ full conversion of propane was observed only at 350°C [22]. It is apparent that our catalyst appears to be among the most active propane combustion catalysts reported thus far.

Fig. 10a shows a long term testing of the catalyst at temperatures of 230 and 200°C . The $\text{Co}_3\text{O}_4\text{-GC-6}$ catalyst exhibited high catalytic activity and stability for at least 50 h at both reaction temperatures. The initial conversion was reduced from 47 to 43% at 200°C may be due to an induction period. Such a decrease in activity is commonly observed with many laboratories and commercial catalysts. To further examine the likely thermal stability of the $\text{Co}_3\text{O}_4\text{-GC}$ material at higher reaction temperatures, an accelerated aging process by cycling the reactor temperature between 210 and 500°C was carried out. As shown in Fig. 10b, it is evident that deactivation had occurred as the conversion at 210°C was reduced to 50% , compared with ca. 74% for the fresh $\text{Co}_3\text{O}_4\text{-GC-6}$ catalyst. It is worth noting that no further deactivation was identified during the second cycle, which may be rationalized by the maintenance of the BET specific surface area (ca. $58 \text{ m}^2 \text{ g}^{-1}$) upon repeated thermal treatment. The activation energies (E_a) derived from the plots

Table 2

Reaction temperature at 10 and 100% propane conversion (T_{10} and T_{100}), reaction rates and activation energies (E_a) for all catalysts.

Catalysts	T_{10}^a ($^\circ\text{C}$)	T_{100}^a ($^\circ\text{C}$)	r_w^b ($\text{g}_{\text{C}_3} \text{ kg}_{\text{cat}}^{-1} \text{ h}^{-1}$)	r_A^c ($\text{mmol}_{\text{C}_3} \text{ m}^{-2} \text{ h}^{-1}$)	E_a (kJ mol^{-1})
$\text{Co}_3\text{O}_4\text{-SG}$	242	360	–	–	58.6 (0.999)
$\text{Co}_3\text{O}_4\text{-CC}$	221	340	18.1	6.3	55.6 (0.998)
$\text{Co}_3\text{O}_4\text{-GC-0.5}$	202	300	119.6	19.9	51.2 (0.999)
$\text{Co}_3\text{O}_4\text{-GC-1}$	195	280	194.37	31.5	49.7 (0.999)
$\text{Co}_3\text{O}_4\text{-GC-3}$	189	270	309.8	48.6	51.4 (0.999)
$\text{Co}_3\text{O}_4\text{-GC-6}$	182	240	587.8	91.3	51.7 (0.998)

^a The temperature at which the conversion was 10 or 100%.

^b Specific activity per cobalt oxide mass unit at 200°C .

^c Specific activity per surface area at 200°C .

Table 3

Comparison of propane total oxidation over nanocrystalline cobalt oxide with catalysts reported in the literature.

Catalyst	Reaction conditions	W/F (g s mL^{-1})	r_w^a ($\text{g}_{\text{C}_3} \text{ kg}_{\text{Co}_3\text{O}_4}^{-1} \text{ h}^{-1}$)	r_A^b ($\text{mmol}_{\text{C}_3} \text{ m}^{-2} \text{ h}^{-1}$)	Ref.
$\text{Co}_3\text{O}_4\text{-GC-6}$	1% C_3H_8 , 10% O_2	0.12	587.8	91.3	This work
Co_3O_4	0.8% C_3H_8 , 20% O_2	0.3	75.4	33.6	[24]
Co_3O_4	2% C_3H_8 , 10% O_2	0.03	94.3 ^c	277 ^c	[49]
Commercial Co_3O_4	0.5% C_3H_8 , 20% O_2	0.3	0.05	0.66	[19]
$\text{Co/Al}_2\text{O}_3$	0.5% C_3H_8 , 20% O_2	0.3	6.0 ^d	0.22 ^d	[19]
$\text{Co/Al}_2\text{O}_3$	1% C_3H_8 , 16% O_2	0.4	3.5 ^d	>0.02 ^d	[22]
Co/TiO_2	0.5% C_3H_8 , 20% O_2	0.3	35.6 ^d	3.3 ^d	[19]
4.8 wt% $\text{Pt/Al}_2\text{O}_3$	1% C_3H_8 , 16% O_2	0.4	79.6 ^e	–	[22]
4.8 wt% $\text{Au/Al}_2\text{O}_3$	1% C_3H_8 , 16% O_2	0.4	207 ^f	–	[22]
5 wt% $\text{Rh/Al}_2\text{O}_3$	5% C_3H_8 , 25% O_2	0.13	548 ^g	–	[23]

^a Mass specific activity calculated at 200°C .

^b Areal specific activity (per m^2 of surface area) calculated at 200°C .

^c Specific activity calculated at 230°C .

^d Specific activity calculated at 300°C .

^e Specific activity that is normalized to platinum mass for this catalyst sample ($\text{g}_{\text{C}_3} \text{ kg}_{\text{Pt}}^{-1} \text{ h}^{-1}$) at 200°C .

^f Specific activity that is normalized to gold mass for this catalyst sample at 395°C ($\text{g}_{\text{C}_3} \text{ kg}_{\text{Au}}^{-1} \text{ h}^{-1}$).

^g Specific activity that is normalized to rhodium mass for this catalyst sample at 350°C ($\text{g}_{\text{C}_3} \text{ kg}_{\text{Rh}}^{-1} \text{ h}^{-1}$).

in Fig. 11 are similar for all the grinding-derived samples (Table 2), indicating almost the same reaction mechanism of total oxidation of propane over all the $\text{Co}_3\text{O}_4\text{-GC}$ catalysts. Moreover, the relatively lower activation energy over the $\text{Co}_3\text{O}_4\text{-GC}$ catalysts (Table 2) compared to the $\text{Co}_3\text{O}_4\text{-SG}$ and $\text{Co}_3\text{O}_4\text{-CC}$ may be related with the very small particle size and unique structural disorder (as shown in the following sections), both of which facilitate the adsorption and activation of the reactants.

The reaction order with respect to the two reactants propane and O_2 was determined on catalyst $\text{Co}_3\text{O}_4\text{-GC-6}$ by varying the concentration of the one component in the gas mixture while keeping the concentration of the other constant (Fig. 12). The calculated order of the propane oxidation reaction was estimated to be 0.63 with respect to propane and 0.45 with respect to O_2 . There are considerable discrepancies in the literature data with respect to the reaction order of propane and O_2 , even for the same catalytic system [47]. This may be caused by the very different experiment conditions. Moro-oka et al. have demonstrated that the propane and O_2 reaction orders over Co_3O_4 catalyst are strongly dependent on the reaction temperature, partial pressure and catalyst preparation method [47]. As reported in literature, the zero order dependence of O_2 concentration suggests that the active oxygen species are the lattice oxygen. In the present study, the fact that 0.45-order in oxygen permits to assume that it is the weakly bound oxygen species which takes part in the reaction and possibly serves as the active species for propane oxidation. It is also interesting to note that the 0.63-order in propane is rather low in comparison with the value of 0.94 obtained by Moro-oka et al. over a coprecipitation-derived Co_3O_4 system [46]. While further work is needed to fully understand the molecular mechanism how C_3H_8 is activated on catalyst surface, it is most likely that the C–H activation may proceed via a homolytic abstraction of hydrogen by surface bound O^- species [48].

3.4. Active sites and structure-activity relationships

Previous studies on cobalt oxide-based catalysts for propane combustion showed that a number of parameters such as the crystallite size, bulk oxygen mobility or reducibility of cobalt species, the nature of support as well as the cobalt content of the catalysts are thought to be of relevance to understand the observed catalytic behavior for the deep oxidation of light alkanes [11,19,49]. Generally, catalyst with high reducibility shows better performance in the combustion of alkanes [19,24]. Therefore, the reaction is believed to occur through a Mars–Van Krevelen mechanism involving

lattice oxygen via a redox cycle [50]. A recent work by Solsona et al. [24] emphasized the key aspect of the reducibility of a series of nanocrystalline cobalt spinel catalysts with different crystallite size in determining the propane combustion activity, in line with

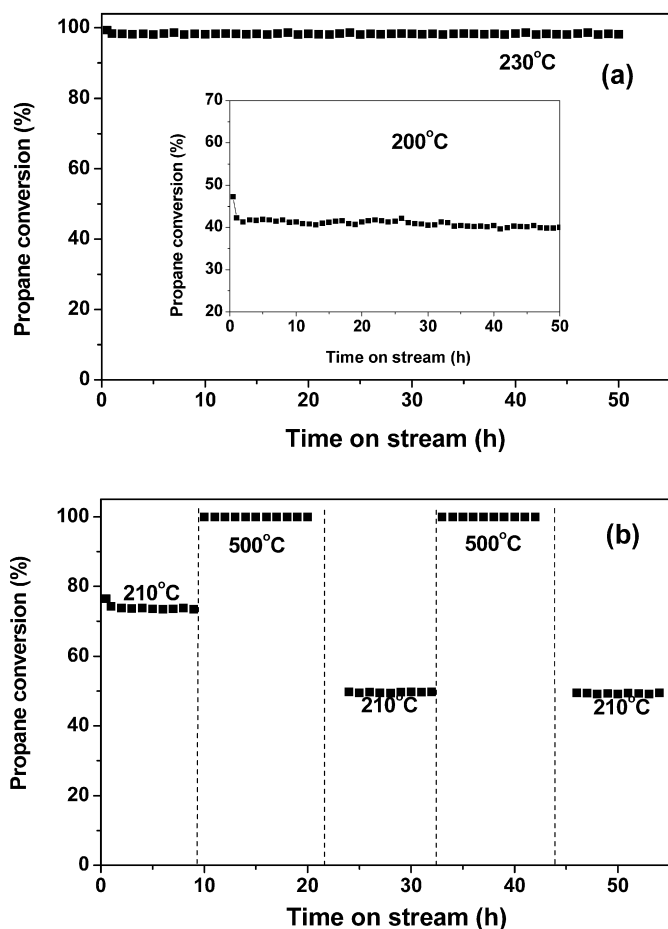


Fig. 10. The stability of Co₃O₄-GC-6 catalyst: (a) 50 h online at 230 or 200 °C and (b) influence of accelerated aging on the propane conversion rates of Co₃O₄-GC-6. (Conditions: catalyst weight = 200 mg. Total volumetric flow = 100 mL min⁻¹).

the apparently low activity of the reference samples as revealed in the present study. However, it is difficult to associate catalyst activity with the different reducibility of cobalt in Co₃O₄-GC samples, since there is no direct relation between the reducibility and the activity of the catalyst for total oxidation of propane. Therefore other factors, rather than the reducibility, may contribute to the high activity of the grinding-derived cobalt oxides.

Alternatively, it is known that hydrocarbon oxidations over metal oxides may occur through a suprafacial reaction mechanism [51,52], which is operative at $T < 400$ °C and involves oxygen species adsorbed over the surface oxygen vacancies of the catalyst. Indeed, we have observed by O₂-TPD the presence of a relevant concentration of superficial oxygen species easily desorbed below 350 °C in all Co₃O₄-GC samples. In order to clarify the dependence of the catalytic activity upon precursor grinding, correlation between the activity of the Co₃O₄-GC catalysts and the integrated peak area of superficial α_1 - or α_2 -oxygen species as determined by O₂-TPD measurements is illustrated in Fig. 13. While the variation of α_2 -oxygen amount shows an excellent correlation with the

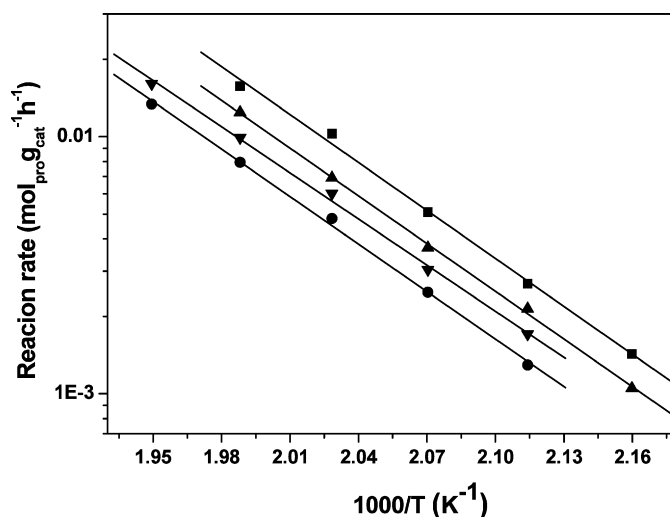


Fig. 11. Arrhenius plots of the temperature dependent reaction rate over Co₃O₄ catalysts. (●) Co₃O₄-GC-0.5, (▼) Co₃O₄-GC-1, (▲) Co₃O₄-GC-3, (■) Co₃O₄-GC-6.

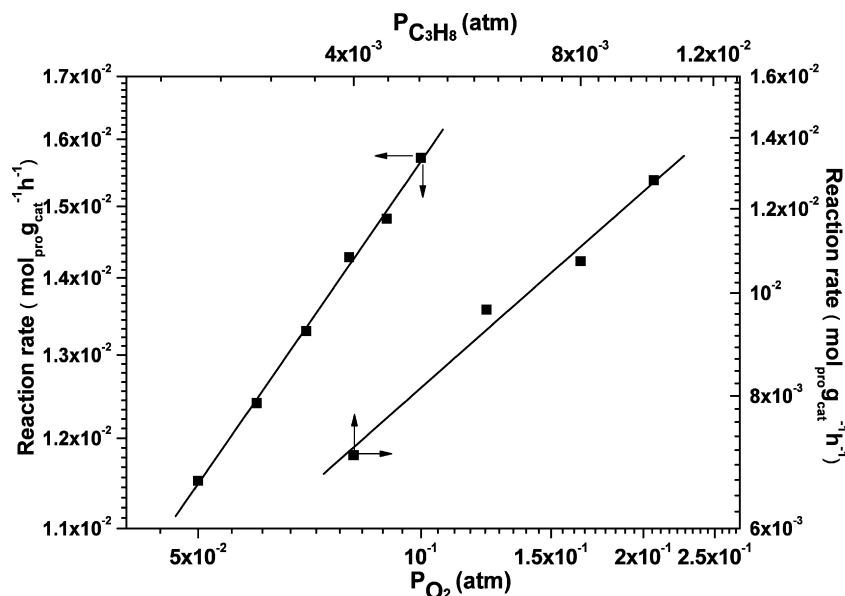


Fig. 12. Determination of the reaction order of propane (0.04–1.2 kPa C₃H₈, 10 kPa O₂, balance N₂) and O₂ (0.5–12 kPa O₂, 1 kPa C₃H₈, balance N₂) in a gas flow of 100 mL min⁻¹ at 230 °C over Co₃O₄-GC-6.

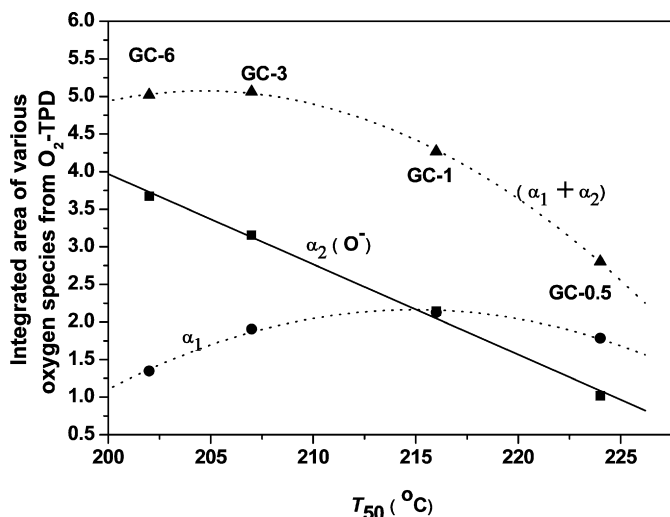


Fig. 13. The signal intensity corresponding to peak α_2 (O^-) as a function of T_{50} for propane oxidation for all the Co_3O_4 -GC-t catalysts.

corresponding combustion activity, a less straightforward relationship was identified between the activity and α_1 -oxygen species. This indicates that the amount of chemisorbed α_2 -oxygen (O^-) is the determining factor leading to high activity and stability of the Co_3O_4 -GC materials. This result, taken together with the essential nature of surface bound O^- species in contributing an efficient electrophilic oxidation reaction [47,53], gives strong evidence the key aspect of active α_2 -oxygen species for propane combustion.

The participation of electrophilic O^- species in cobalt oxide-based catalysts for hydrocarbon oxidation has been reported so far [52]. In this context, it has been suggested that the structural defects of the spinel lattice play a key role in creating active sites on the surface [54], which might play an important favorable role in accelerating the activation and dissociation of oxygen molecules leading to the formation of chemisorbed O^- species. These situations are usually reached by an incorporation of other metals into the lattice, which can create a higher density of oxygen defect sites easily accessible to reactants [55]. At this juncture, it is interesting to point out that the present dry citrate-based SRG process can allow the effective creation of highly strained Co_3O_4 nanocrystals with enhanced lattice distortion in a much simpler manner, which is responsible for the favorable creation of significantly higher amount of O^- species on the surface of the final material (Fig. 7). This may well account for the improved propane combustion activity of the Co_3O_4 -GC catalysts as compared to conventionally prepared cobalt oxide. In this respect, it appears that in order to obtain more active catalysts for propane combustion one should achieve a higher lattice strain level in the Co_3O_4 -based catalysts.

4. Conclusion

This study demonstrates that nanocrystalline cobalt oxides prepared by citrate-precursor-based soft reactive grinding procedure are exceptionally active for total oxidation of light hydrocarbons. Kinetic results show that these grinding-derived cobalt spinel catalysts are among the most active catalysts yet reported for propane combustion, being considerably more active than the previously best reported catalytic activity of cobalt-based catalysts for complete hydrocarbon removal. The superior activity of the present grinding-derived cobalt oxide catalyst has been attributed to the beneficial formation of highly strained cobalt spinel nanocrystals as a consequence of prolonged mechanochemical activation during the dry citrate-precursor synthesis process.

Acknowledgments

This work was supported by the National Natural Science Foundation of China (20633030, 20721063 and 20873026), the National Basic Research Program of China (2003CB615807), the National High Technology Research and Development Program of China (2006AA03Z336), the Committee of the Shanghai Education (06SG03) and the Committee of Shanghai Science and Technology (07QH14003).

References

- [1] G.L. Bezemer, U. Falke, A.J.V. Dillen, K.P.D. Jong, Chem. Commun. 6 (2005) 731.
- [2] F. Morales, D. Grandjean, F.M.D. Groot, O. Stephan, B.M. Weckhuysen, Phys. Chem. Chem. Phys. 7 (2005) 568.
- [3] M.J. Pollard, B.A. Weinstock, T.E. Bitterwolf, P.R. Griffiths, A.P. Newbery, J.B. Paine, J. Catal. 254 (2008) 218.
- [4] H. Tüysüz, M. Comotti, F. Schüth, Chem. Commun. 34 (2008) 4022.
- [5] U. Chellam, Z.P. Xu, H.C. Zong, Chem. Mater. 12 (2000) 650.
- [6] J. Llorca, P.R.D.I. Piscina, J.A. Dalmon, N. Homs, Chem. Mater. 16 (2004) 3573.
- [7] L.B. Backman, A. Rautiainen, M. Lindblad, O. Jylhä, A.O.I. Krause, Appl. Catal. A 208 (2001) 223.
- [8] J. Petryk, E. Kolakowska, Appl. Catal. B 24 (2000) 121.
- [9] T. Ataloglou, J. Vakros, K. Bourikas, C. Fountzoula, C. Kordulis, A. Lycourghiotis, Appl. Catal. B 57 (2005) 299.
- [10] M. Dhakad, T. Mitsuhashi, S. Rayalu, P. Doggali, S. Bakardjiva, J. Subrt, D. Fino, H. Hameda, N. Labhsetwar, Catal. Today 132 (2008) 188.
- [11] E. Finocchio, G. Busca, V. Lorenzelli, V.S. Escribano, J. Chem. Soc. Faraday Trans. 92 (1996) 1587.
- [12] T.V. Choudhary, S. Banerjee, V.R. Choudhary, Appl. Catal. A 234 (2002) 1.
- [13] W. Yue, A.H. Hill, A. Harrison, W.Z. Zhou, Chem. Commun. 24 (2007) 2518.
- [14] Y. Minato, K. Aoki, M. Shirai, M. Arai, Appl. Catal. A 209 (2001) 79.
- [15] S.G. Christoskova, M. Stoyanova, M. Georgieva, D. Mehandjiev, Mater. Chem. Phys. 60 (1999) 59.
- [16] A. Miyamoto, T. Ui, Y. Murakami, J. Catal. 88 (1984) 526.
- [17] D. Pope, D.S. Walker, R.L. Moss, J. Catal. 47 (1977) 33.
- [18] J.A. Schwarz, Chem. Rev. 95 (1995) 477.
- [19] B. Solsona, I. Vázquez, T. García, T.E. Davies, S.H. Taylor, Catal. Lett. 116 (2007) 116.
- [20] I. Yuranov, N. Dunand, L. Kiwi-Minsker, A. Renken, Appl. Catal. B 36 (2002) 183.
- [21] M. Paulis, L.M. Gandia, A. Gil, J. Sambeth, J.A. Odriozola, M. Montes, Appl. Catal. B 26 (2000) 37.
- [22] A.C. Gluhoi, N. Bogdanchikova, B.E. Nieuwenhuys, Catal. Today 113 (2006) 178.
- [23] A.F. Lee, C.R. Seabourene, K. Wilson, Catal. Commun. 7 (2006) 566.
- [24] B. Solsona, T.E. Davies, T. García, I. Vázquez, A. Dejoz, S.H. Taylor, Appl. Catal. B 84 (2008) 176.
- [25] B.P.G. McCormick, T. Tsuzuki, J.S. Robinson, J. Ding, Adv. Mater. 13 (2001) 1008.
- [26] R.D. Zhang, A. Villanueva, H. Alamdari, S. Kaliaguine, Appl. Catal. B 64 (2006) 220.
- [27] L.C. Wang, Y.M. Liu, M. Chen, Y. Cao, H.Y. He, G.S. Wu, W.L. Dai, K.N. Fan, J. Catal. 246 (2007) 193.
- [28] H.P. Klug, L.E. Alexander, X-Ray Diffraction Procedures, Wiley, New York, 1954.
- [29] B.L. Knier, T. Ressler, A. Rabis, F. Girgsdies, M. Baenitz, F. Steglich, R. Schlögl, Angew. Chem. Int. Ed. 43 (2004) 112.
- [30] Q. Liu, L.C. Wang, M. Chen, Y.M. Liu, Y. Cao, H.Y. He, K.N. Fan, Catal. Lett. 121 (2008) 144.
- [31] I. Lopes, N.E. Hassan, H. Guerba, G. Wallez, A. Davidson, Chem. Mater. 18 (2006) 5826.
- [32] C.F. Windisch, G.J. Exarhos, J. Appl. Phys. 95 (2004) 5435.
- [33] L. He, Z.C. Li, Z.J. Zhang, Nanotechnology 15 (2008) 155606.
- [34] P. Arnoldy, J.A. Moulijn, J. Catal. 93 (1985) 38.
- [35] M. Kang, M.W. Song, C.H. Lee, Appl. Catal. A 251 (2003) 143.
- [36] C.W. Tang, C.C. Kuo, M.C. Kuo, C.B. Wang, S.H. Chien, Appl. Catal. A 309 (2006) 37.
- [37] L. Xue, C. Zhang, H. He, Y. Teraoka, Appl. Catal. B 75 (2007) 167.
- [38] L. Spadaro, F. Arena, M.L. Granados, M. Ojeda, J.L.G. Fierro, F. Frusteri, J. Catal. 234 (2005) 451.
- [39] C.W. Tang, W.Y. Yu, C.J. Lin, C.B. Wang, S.H. Chien, Catal. Lett. 116 (2007) 161.
- [40] M. Meng, P.Y. Lin, Y.I. Fu, Catal. Lett. 48 (1997) 213.
- [41] N.A. Merino, B.P. Barbero, P. Grange, L.E. Cadús, J. Catal. 231 (2005) 232.
- [42] W. Ding, Y. Chen, X. Fu, Catal. Lett. 23 (1994) 69.
- [43] S.G. Christoskova, M. Stoyanova, M. Georgieva, D. Mehandjiev, Mater. Chem. Phys. 60 (1999) 39.
- [44] M. Moroney, R.S.C. Smort, M.W. Roberts, J. Chem. Soc. Faraday Trans. 79 (1983) 1769.
- [45] M.A. Langell, F. Gevrey, M.W. Nydegger, Appl. Surf. Sci. 153 (2000) 114.
- [46] M.R. Morales, B.P. Barbero, L.E. Cadús, Appl. Catal. B 74 (2007) 1.
- [47] A. Bielanski, J. Haber, Oxygen in Catalysis, Dekker, New York, 1991.
- [48] Y. Moro-oka, Y. Morikawa, A. Ozaki, J. Catal. 7 (1967) 23.
- [49] G. Busca, M. Daturi, E. Finocchio, V. Lorenzelli, G. Ramis, R.J. Willey, Catal. Today 33 (1997) 239.

- [50] K.S. Song, D. Klvana, J. Kirchnerova, Appl. Catal. A 213 (2001) 113.
- [51] R.J.H. Voorhoeve, J.P. Remeika, L.E. Trimble, Acad. Sci. 2 (1976) 272.
- [52] Y.Z. Wang, Y.X. Zhao, C.G. Gao, D.S. Liu, Catal. Lett. 125 (2008) 134.
- [53] G. Tulyev, S. Angelov, Appl. Surf. Sci. 32 (1988) 381.
- [54] M. Machida, Y. Murata, K. Kishikawa, D.J. Zhang, K. Ikeue, Chem. Mater. 20 (2008) 4489.
- [55] J.L. Gautier, E. Rios, M. Gracia, J.F. Marco, J.R. Gancedo, Thin Solid Films 311 (1997) 51.